


Please cite the Published Version

Nederveen, Joshua P, Joannis, Sophie , Thomas, Aaron CQ, Snijders, Tim, Manta, Katherine, Bell, Kirsten E, Phillips, Stuart M, Kumbhare, Dinesh and Parise, Gianni (2020) Age-related changes to the satellite cell niche are associated with reduced activation following exercise. The FASEB Journal, 34 (7). pp. 8975-8989. ISSN 0892-6638

DOI: <https://doi.org/10.1096/fj.201900787r>

Publisher: Wiley

Version: Accepted Version

Downloaded from: <https://e-space.mmu.ac.uk/626411/>

Usage rights:  In Copyright

Additional Information: This is an Author Accepted Manuscript of a paper accepted for publication in The FASEB Journal, published by and copyright Wiley.

Enquiries:

If you have questions about this document, contact openresearch@mmu.ac.uk. Please include the URL of the record in e-space. If you believe that your, or a third party's rights have been compromised through this document please see our Take Down policy (available from <https://www.mmu.ac.uk/library/using-the-library/policies-and-guidelines>)

Title:

Age-related incarceration of satellite cells is associated with their reduced activation following exercise stimulus

Authors and institutions:

Joshua P Nederveen¹, Sophie Joannis¹, Aaron CQ Thomas¹, Tim Snijders^{1,3}, Katherine Manta¹, Kirsten E. Bell¹, Stuart M Phillips¹, Dinesh Kumbhare², Gianni Parise^{1,*}

Departments of ¹Kinesiology, ²Medicine McMaster University, Hamilton, Ontario, Canada, L8S 4L8, ³ Human Biology, NUTRIM School of Nutrition and Translational Research in Metabolism, Maastricht University Medical Center+, Maastricht, the Netherlands.

Corresponding author

*Departments of Kinesiology , McMaster University, Hamilton, Ontario, Canada L8S 4L8. E-mail: parise@mcmaster.ca; Telephone: 905 525 9140 ext. 27353

Running Title:

Incarcerated satellite cells have less activation

NONSTANDARD ABBREVIATIONS

Analysis of variance; ANOVA

Cross-sectional area; CSA

Dual-energy X-ray absorptiometry; DEXA

Extracellular matrix; ECM

Nonsteroidal anti-inflammatory drugs; NSAID

Older men under training and/or acute exercise conditions; OM-Ex

Older men; OM

Optimal Cutting Temperature compound; OCT

Region of interest; ROI

Repetition max; RM

Satellite cell; SC

Young men; YM

ABSTRACT

Skeletal muscle satellite cell (SC) function and responsiveness is regulated, at least in part, through interactions within the niche in which they reside. Evidence suggests that structural changes occur in the SC niche as a function of aging. In the present study, we investigated the impact of aging on SC niche properties. Muscle biopsies were obtained from the *vastus lateralis* of healthy young (YM; 21±1yr;n=10) and older men (OM; 68±1yrs;n=16) at rest. A separate group of older men (OM-Ex; 73±1;n=24) performed a single bout of resistance exercise and additional muscle biopsies were taken 24 and 48h post-exercise; this was performed before and following 12wks of combined exercise training. Muscle SC niche measurements were assessed using high resolution immunofluorescent confocal microscopy. Type II SC niche laminin thickness was greater in OM (1.86±0.06µm) as compared to YM (1.55±0.09µm, p<0.05). The percentage of type II-associated SC that were incarcerated by laminin was greater in OM (13.6±4.2%) as compared to YM (3.5±1.5%; p<0.05). In non-incarcerated SC, the proportion of active MyoD⁺/Pax7⁺ SC were higher compared to incarcerated SC (p<0.05) following a single bout of exercise. Incarceration of the SC niche by laminin appears with aging and may inhibit SC activation in response to exercise.

KEY WORDS: muscle stem cells, Pax7, basal lamina, satellite cell niche

INTRODUCTION

The age-related decline in skeletal muscle mass and strength, termed sarcopenia, has a broad impact on elderly individuals, manifesting as impaired physical function, elevated rates of disability and reduced quality of life. The progressive loss of muscle size has been primarily attributed to a decline in type II muscle fibre size (Verdijk *et al.*, 2007; Nilwik *et al.*, 2013), occurring along with a reduction in skeletal muscle satellite cell (SC) content (Verdijk *et al.*, 2007, 2014). SC are anatomically located beneath the basal lamina and outside the sarcolemma (Mauro, 1961), are required for muscle repair following myotrauma (Lepper *et al.*, 2011; McCarthy *et al.*, 2011; Sambasivan *et al.*, 2011), and are responsive to resistance exercise. Following activation, SC proliferate and terminally differentiate donating their nuclei to existing myofibres to support repair, regeneration or maintenance of muscle. With aging, consistent with a relative resistance to anabolic stimuli, there is a blunted SC activation which is accompanied by a delay in the type II muscle SC response (McKay *et al.*, 2012; Snijders *et al.*, 2014). Given the importance of the addition of new myonuclei to maintain muscle health, a reduction in SC number and/or function in response to physiological stimuli has been proposed to be an important factor in the development of sarcopenia (Snijders *et al.*, 2015). The environment in which the SC resides is known as the SC niche. The SC niche is composed of the basal lamina, the sarcolemma, the extracellular matrix (ECM) and the fibre to which the SC is associated, making the niche an important factor in the efficient regulation of the SC response. Recent evidence suggests that SC can be regulated through multiple mechanisms including: endocrine growth factors, paracrine factors from adjacent muscle fibres (Pedersen & Febbraio, 2008), local coordination amongst muscle resident cells (i.e., endothelial cells, inflammatory cells) (Christov *et al.*, 2007; Joe *et al.*, 2010) and through biophysical characteristics of the niche (Bentzinger *et al.*, 2013; Garg & Boppart, 2016).

Age-related biophysical modifications of the SC niche may be related to an impaired myogenic response, potentially altering the capacity for muscle repair. The ECM, an important component of the SC niche, provides structural integrity and clearly defines the SC niche borders from other muscle resident cells and interstitial matrix (McCarthy & Hay, 1991; Urciuolo *et al.*, 2013; Thomas *et al.*, 2015). The ECM can also provide regulatory cues to the SC to maintain quiescence or, alternatively, become activated (Thomas *et al.*, 2015). Evidence suggests that

there is a thickening of the basal lamina with aging, including a marked increase in thickness and alterations in structure and alignment (Candiello *et al.*, 2010). The physical association between SC and the myofibre can be inhibited by a thickening of the basal lamina and/or increased collagen deposition (Snow, 1977). These structural changes to aspects of the inner basal lamina, with changing proportions of nonfibrillar collagen and laminin have been observed to occur in a fibre-type specific manner in rats (Kovanen *et al.*, 1988), however there is limited literature in regard to the changing profile of the SC niche within the context of human aging. The changes in the composition of the SC niche that occur with aging may subsequently lead to impaired SC function. Therefore, in the present study we assessed: i) the collagen content of skeletal muscle, and using confocal microscopy; ii) basal lamina and SC niche thickness and composition in healthy young and older men. We hypothesized that the thickness and composition of the SC niche would be altered in older as compared to young men.

MATERIALS AND METHODS

Participants. Ten healthy young men (YM: 21 ± 1.0 yr; means \pm SEM) and a total of 40 healthy older men comprising two separate groups (OM: $n = 16$, 68 ± 1 yr; OM-Ex: $n = 24$, 73 ± 1 yr; mean \pm SEM) were recruited to participate in this study. Subjects did not participate in any type of structured exercise programme for ≥ 4 months prior to the study and were required to complete a routine screening and health questionnaire. Exclusion criteria included smoking, diabetes, the use of nonsteroidal anti-inflammatory drugs (NSAIDs) and/or simvastatin, and history of respiratory disease and/or any major orthopaedic disability. Throughout their participation in this trial, subjects were told to refrain from any exercise unrelated to the study. The study was approved by the Hamilton Health Sciences Integrated Research Ethics Board and conformed to the guidelines outlined in the Declaration of Helsinki. Participants gave their informed written consent prior to their inclusion to the study.

Muscle biopsy sampling. Percutaneous needle biopsies were taken from the mid-portion of the vastus lateralis muscle under local anaesthetic using a custom-modified 5-mm Bergstrom needle adapted for manual suction under local anaesthesia (2% xylocaine) following an (~10h) overnight fast. Subjects reported to the laboratory during in morning and a biopsy was taken for baseline analysis (Pre). Subjects had not participated in any physical activity for at least 96 hours before the biopsy collection. In an additional group of older men that performed the 12 wk

exercise training (OM-Ex: n = 24), two additional muscle biopsies were taken from the alternating legs, 24 and 48 h after a single session of resistance exercise. The Pre-, 24h-post and 48h-post exercise biopsies were repeated both prior to (PRE; before chronic training) and following the 12 wk exercise training program (POST; following chronic training). Consecutive muscle biopsy sampling was alternated between legs. The leg in which the baseline biopsy was drawn from was randomized. Incisions for the repeated muscle biopsy sampling were spaced by approximately 3 cm to minimize any effect of the previous biopsy. Upon excision, all muscle biopsy samples were immediately mounted in optimal cutting temperature (OCT) compound, frozen in liquid nitrogen-cooled isopentane, and stored at -80° C until further analysis.

Familiarization and baseline testing. One week prior to any baseline biopsy or acute bout of exercise, subjects visited the laboratory for the following: DEXA scan (previously reported in Bell *et al.* 2017) and a familiarization session with biopsy procedures. For the exercise group, proper lifting technique was demonstrated and practiced by participants during a familiarization session. Muscle strength was assessed using 1RM strength tests and was performed on weight machines for leg extension (Atlantis Precision Series Leg Extension C-105, Laval QC) and leg press (HUR 3545 Leg Press Incline: HUR, Northbrook, IL, USA).

Acute exercise protocol. To determine SC activation status, the OM-Ex group performed a single bout of resistance exercise. In short, the OM-Ex performed a session of exercise that consisted of four sets of 10 repetitions each at 65% of 1RM on leg press, chest press, horizontal row and leg extension. Exercise was performed under personal supervision, all participants were verbally encouraged during the exercise and the final set of each exercise was performed to volitional failure, which was defined as the inability to complete an additional repetition with proper form. A resting period of 2 min between sets was allowed. Prior to and following the resistance exercise, a 5 min warm up/cool down was performed on a cycle ergometer. The resistance-type exercise protocol was based on previous work that showed that either concentric and/or eccentric muscle contractions are sufficient to cause an expansion of the SC pool and are well tolerated by participants (McKay *et al.*, 2012; Nederveen *et al.*, 2018).

Long term exercise protocol over 12-wks. To determine changes to the SC niche with chronic exercise, the OM-Ex group performed a structured exercise program. Exercise training was performed three times per week, comprised of two resistance and one high intensity interval

training session under strict supervision as described previously (Snijders *et al.*, 2019). Briefly, resistance exercise consisted of a five min warm-up on cycle ergometer, followed by three sets (10 repetitions per set at 80% 1RM) of four separate exercises in the following order: leg press, chest press or lateral pull-down, horizontal row or shoulder press, and leg extension. Chest press and horizontal row were only performed on Monday and lateral pull-down and shoulder press were only performed on Friday (leg press and leg extension were performed at every resistance exercise session). To maintain a sufficient training stimulus and account for adaptations, workload was increased when more than eight repetitions could be performed in the third set of the exercise. Interval sessions were performed on a cycle ergometer (ISO1000 Upright Bike; SCIFIT, Tulsa, OK) while wearing a heart rate monitor (H7 Heart Rate Sensor; Polar Electro Canada, Lachine, QC). Following three minutes warmup at 25 W, participants completed 10 x 60 s intervals at a workload which elicited ~90% maximal heart rate, while maintaining a cadence of ≥ 90 rpm. Workload was adjusted as needed to maintain an average heart rate of ~90% heart rate max over the 10 intervals.

Immunofluorescence. Muscle cross sections (7 μ m) were prepared from unfixed OCT embedded samples, stored at -80°C. Samples were stained with antibodies against appropriate primary and secondary antibodies, found in Table 1, as previously described (Nederveen *et al.*, 2016, 2018). Nuclei were labelled with DAPI (4',6-diamidino-2-phenylindole) (1:20000, Sigma-Aldrich, Oakville, ON, Canada), prior to cover slipping with fluorescent mounting media (DAKO, Burlington, ON, Canada). The staining procedures were verified using negative controls, in order to ensure appropriate specificity of staining. Slides were viewed with the Nikon Eclipse *Ti* Microscope (Nikon Instruments, Inc. USA), equipped with a high-resolution Photometrics CoolSNAP HQ2 fluorescent camera (Nikon Instruments, Melville, NY, USA). Images were captured and analyzed using the Nikon NIS Elements AR 3.2 software (Nikon Instruments, Inc., USA). For confocal microscopy, all images were obtained with the 60x Plan Apochromat 60x/1.4 objective oil immersion objective using the Nikon C2+ confocal microscopy (Nikon Instruments, Melville, NY, USA), featuring the Nikon LU-N4 laser system (Nikon Instruments, Melville, NY, USA) for laser excitations for the various fluorophores.

In the OM and YM groups, SC incarceration was defined as the lamina covering ≥ 90 % of the perimeter of the Pax7+/DAPI+ cell (Figure 1A-E provides an example of laminin staining

surrounding a SC, constituting what we have termed ‘incarceration’. Figure 1F-J provides an example of a non-incarcerated SC and a similar presentation to previous work from our group (Nederveen et al. 2017, Joannis et al. 2015, McKay et al. 2012). We have termed this status ‘incarceration’ because it would appear that these SC are associated with the laminin in a novel way (i.e., being completely enclosed by it) compared to previous observations (i.e., with SC lying simply beneath the basal lamina). Please refer to Figure 1 for differentiation between these two SC-laminin associations. For fibre type specific SC basal lamina thickness, a total of $n = 368$ SC (OM: 182; YM: 186) were included in the analysis (Pax7/Laminin/DAPI/MHCI). The thickness of the laminin was acquired by taking the average of three measurements across the basal lamina surrounding each SC. SC on the periphery of sections were not included in the analysis. For the SC niche CSA (Pax7/Laminin/Desmin/DAPI) a total of $n = 344$ SC (OM: $n = 177$; YM = 167) were included. SC anatomical niche measurements were determined via separated immunofluorescent staining. In brief, Pax7⁺/DAPI⁺ cells were located beneath the basal lamina via confocal microscopy, and the area between the desmin positive area and the basal lamina itself was identified as the SC niche cross-sectional area (CSA). The cross-sectional area of the SC nuclei (SC nuc-CSA) was determined by quantifying the area (μm^2) of the DAPI⁺ signature of the individual Pax7⁺/DAPI⁺ cell.

In the OM-Ex group, SC incarceration was determined in a similar fashion, but included the following cell populations: quiescent (i.e., Pax7⁺/MyoD⁻), and activated (i.e., Pax7⁺/MyoD⁺). A total of $n = 646$ SC (Pre: 189; 24h: 249; 48h: 209 SC) were included in the analysis in the PRE condition (prior to 12 wk exercise training) and a total of $n = 1348$ SC (Pre: 466; 24h: 498; 48h: 368 SC) were included in the analysis in the POST condition (following 12 wk chronic training).

Colour microscopy. Masson’s trichrome stain was used to determine collagen content in muscle cross-sections. Sections were fixed in 4% PFA for 1 h, then incubated in Bouin’s fixative (Sigma-Aldrich, St. Louis, MO, USA) overnight at room temperature. Slides were rinsed in water, incubated in Weigert’s iron hematoxylin for 5 min, washed again, and incubated in Biebrich scarlet-acid fuchsin for 15 min. Slides were then rinsed in water, incubated in phosphomolybdic-phosphotungstic acid (3×3 min), incubated in aniline blue, dipped in water, and incubated in 1% glacial acetic acid for 2 min. Slides were treated with graded ethanol washes, then cover-slipped. The area occupied by collagen (stained blue) was determined and

represented as a percentage of total area. Images were taken at $\times 20$ by using Nikon DS-Fi1. To determine the extent of fibrosis, the area occupied by blue staining was determined and expressed as a percentage of total area. Specifically, the blue area was selected via thresholding individually on each RGB image by using Nikon NIS-Elements 3.2 AR software. Thresholding was set using the 6-point circle tool by manually choosing the lightest and darkest blue areas in an image. All colour microscopy analysis was completed in a blinded fashion.

RNA Isolation. RNA was isolated from 15–25 mg of muscle using the Trizol/RNeasy method. All samples were homogenized with 1 mL of Trizol Reagent (Life Technologies, Burlington, ON, Canada), in Lysing Maxtrix D tubes (MP Biomedicals, Solon, OH, USA), with the FastPrep-24 Tissue and Cell Homogenizer (MP Biomedicals, Solon, OH, USA) for a duration of 40 sec at a setting of 6 m/sec. Following a five-minute room temperature incubation, homogenized samples were stored at -80°C for one month until further processing. After thawing on ice, 200 μl of chloroform (Sigma-Aldrich, Oakville, ON, Canada) was added to each sample, mixed vigorously for 15 sec, incubated at RT for 5 min, and spun at 12000 g for 10 min at 4°C . The RNA (aqueous) phase was purified using the E.Z.N.A. Total RNA Kit 1 (Omega Bio-Tek, Norcross, GA, USA) as per manufacturer's instructions. RNA concentration (ng/ml) and purity (260/280) was determined with the Nano-Drop 1000 Spectrophotometer (Thermo Fisher Scientific, Rockville, MD, USA).

Reverse Transcription. Samples were reverse transcribed using a high capacity cDNA reverse transcription kit (Applied Biosystems, Foster City, CA, USA) in 20 μl reaction volumes, as per manufacturer's instructions, using an Eppendorf Mastercycler epGradient Thermal Cycler (Eppendorf, Mississauga, ON, Canada) to obtain cDNA for gene expression analysis.

Quantitative real time RT-PCR. All QPCR reactions were run in duplicate in 25 μl volumes containing RT Sybr Green qPCR Master Mix (Qiagen Sciences, Valencia, CA, USA), prepared with the epMotion 5075 Eppendorf automated pipetting system (Eppendorf, Mississauga, ON, Canada), and carried out using an Eppendorf Realplex2 Master Cycler epgradient (Eppendorf, Mississauga, ON, Canada). Primers are listed in Table 2 and were re-suspended in 1X TE buffer (10mM Tris-HCl and 0.11 mM EDTA) and stored at -20°C prior to use. Changes in messenger RNA (mRNA) gene expression were analysed using the $2^{-\Delta\Delta\text{Ct}}$ method, as previously described

(Schmittgen & Livak, 2008). Briefly, Ct values were first normalized to the housekeeping gene glyceraldehyde 3-phosphate dehydrogenase (GAPDH) (Table 2); GAPDH expression was not different in OM as compared to YM. Ct values were normalized to GAPDH and expressed as arbitrary units.

Immunoblotting methods. Approximately ~20mg of powdered muscle tissue was homogenized in 200 μ l of ice-cold RIPA buffer (89901, Thermo Fisher Scientific, Waltham, Massachusetts, USA) with complete Mini-Protease and Phosphatase Inhibitor Cocktail (78446, Thermo Fisher) using the FastPrep 24 5G (MP Biomedicals, Santa Ana, California, USA) at a speed of 6 m/s for 40 seconds and repeated 3 times. Samples were then centrifuged at 4°C at a speed of 10000 g for 10 minutes to remove insoluble material. Protein content was determined using the BCA assay using a plate reader at an absorbency of 562 nm. Laemmli sample buffer (4X) was added to samples, equal amounts of protein were separated on either 8 – 12.5% gels (Bio-Rad) or 10% resolving gels at 100V for 2 hours, with pre-stained molecular weight standards (Sigma-Aldrich Co., St. Louis, Missouri, USA). Proteins were transferred to nitrocellulose membranes (Trans-Blot® Turbo™ Midi Nitrocellulose (0.2 μ m) Transfer Packs, Bio-Rad) via turbo-blot transfer (Trans-Blot Turbo Transfer System, Bio-Rad) at 25 V for 15 mins. Membranes were stained with Ponceau S (P7170-1L, Sigma-Aldrich) and imaged to assure even loading and for future normalization. Membranes were blocked in 5% dry-milk in tris-buffered saline with tween (TBST) for one hour prior to an overnight primary antibody incubation at 4°C. All primary antibodies were prepared in 5% milk in TBST. All antibodies were used at a concentration of 1:1000 information in Table 1. Membranes were washed in TBST three times prior to incubation in appropriate horse radish peroxidase-conjugated secondary antibody at room temperature for one hour, at a 1:10000 concentration. Membranes were then washed in TBST three times prior to antibody detection. For protein detection, we used a chemiluminescence kit (Clarity™ Western ECL Max™ Blotting Substrates) and the signals were captured with ChemiDoc™ XRS+ System (Bio-Rad). Optical density (O.D.) of the western blotting bands was quantified using Image Lab. Total band volume was determined for each band. All bands were normalized to a gel control when needed in addition to the corresponding ponceau image. Statistical analysis was carried out on normalized values for each protein of interest.

Cell culture, migration assay. C2C12 (ATCC) were maintained at 37°C in 5% CO₂ and cultured in growth media (GM, DMEM supplemented with 10% fetal bovine serum and 1% penicillin streptomycin, Gibco) or serum free media (DMEM only). Similar to previous methods transwell assays were conducted using C2C12 myoblasts using 24 well, 8 µm pore transwell systems, specifically Nunc Polycarbonate Cell Culture Inserts (Thermo Fisher Scientific, Waltham, Massachusetts, USA). Transwells were pre-coated for 2 hours with 100 µl of Matrigel Basement Membrane Matrix containing extracellular matrix proteins, including laminin, collagen IV, heparin sulfate proteoglycans, entactin/nidogen, and a number of growth factors (Corning Scientific, Corning, New York, USA) at varying concentrations in a gradient (100, 200, 400 to 800 ([µg/mL]). 30 000 cells resuspended in serum free media were added to each transwell. 650 µl of serum free media (CTL) or DMEM supplemented with 20% fetal bovine serum was added to the bottom well. Cells were allowed to migrate for 14 hours. Migration was assessed by staining cells with DAPI, removing the cells on the upper side of the transwell and counting the number of migrated cells in 27 fields of view at 20X magnification Nikon Eclipse *Ti* Microscope (Nikon Instruments, Inc. USA), equipped with a high-resolution Photometrics CoolSNAP HQ2 fluorescent camera (Nikon Instruments, Melville, NY, USA).

Statistical analysis. Statistical analysis was performed using Sigma Stat 3.1.0 analysis software (Systat Software, Chicago, IL, USA). Baseline comparisons of fibre type specific muscle characteristics between YM and OM were performed via one-way ANOVA. In addition, to compare the difference in ‘mixed’ fibre type (i.e., where no fibre type specific analysis is possible) muscle SC niche characteristics, nuclear cross-sectional area, fibrotic index, collagen content and fibrosis-related mRNA gene content, a Student’s *t* test was utilized. In order to assess the impact of SC incarceration on SC activation, one-way repeated measures ANOVA were performed separately for the incarcerated and non-incarcerated SC (expressed as a percentage within the two cell populations: quiescent (i.e., Pax7⁺/MyoD⁻), and activated (i.e., Pax7⁺/MyoD⁺). In these one-way repeated measures ANOVA design for the acute response, post-exercise time points were only compared with baseline (Pre) and Bonferonni corrections were applied to account for multiple comparisons. Comparisons of SC activity between incarcerated and non-incarcerated SC at Pre, 24, and 48h were performed via Student’s *t* test. Statistical significance was accepted at $p < 0.05$. All results are presented as means ± standard error of the mean (SEM).

RESULTS

Comparison between OM and YM in a basal state:

Physical characteristics: By design, the age of the OM (68 ± 1 yrs) was significantly greater than the YM (20 ± 1 yrs) ($p < 0.05$). There were no significant differences between OM and YM in height (1.75 ± 0.02 m and 1.78 ± 0.02 m respectively), weight (87.4 ± 3.0 kg and 82.2 ± 4.2 kg, respectively) or BMI (28.8 ± 0.96 kg/m² and 25.8 ± 1.1 kg/m² respectively,).

Indices of fibrosis and collagen composition in mixed fibre type muscle: In OM, the fibrotic index as measured by Masson's trichrome staining was greater (3.6 ± 0.5 %) at baseline, as compared to YM (2.0 ± 0.5 %; $p < 0.05$, Figure 2C).

Gene expression measured at baseline: There were no significant differences in *COL1 α 1* mRNA expression in OM (0.7 ± 0.2 a.u) as compared to YM (0.9 ± 0.2 a.u). There were no significant differences in *COL3 α 1* mRNA expression in OM (4.4 ± 0.9 a.u) as compared to YM (3.3 ± 0.7 a.u). There were no significant differences in *COL4 α 1* mRNA expression in OM (5.9 ± 1.2 a.u) as compared to YM (4.2 ± 0.7 a.u). *COL6 α 1* mRNA expression was not different in OM (4.5 ± 0.6 a.u) as compared to YM (3.6 ± 0.4 a.u). Laminin subunit α 1 and subunit β 1 mRNA expression was significantly greater in OM (2.5 ± 0.6 a.u, 6.2 ± 0.6 a.u., respectively) as compared to YM (1.0 ± 0.2 a.u, 3.4 ± 0.3 a.u., respectively, $p < 0.05$, Figure 2). Laminin subunit γ 1 mRNA expression was not different in OM (1.4 ± 0.2 a.u) compared to YM (1.4 ± 0.3 a.u). MMP-2 mRNA expression was significantly greater in OM (3.1 ± 0.8 a.u) as compared to YM (1.2 ± 0.2 a.u, $p < 0.05$, Figure 2).

Anatomical description of the SC niche: In mixed fibre type muscle, SC niche laminin thickness was greater in OM (1.89 ± 0.04 μ m) as compared to YM (1.62 ± 0.10 μ m, $p < 0.05$). SC niche CSA tended to be larger in OM (25.16 ± 0.49 μ m²) as compared to YM (22.50 ± 1.27 μ m², $p = 0.07$). The percentage of SC in mixed fibre type muscle that were incarcerated by laminin was significantly greater in OM (19.0 ± 1.6 %) as compared to YM (7.2 ± 2.1 %; $p < 0.05$). When separated in a fibre-type specific manner, type I SC niche laminin thickness was not significantly different between OM (1.91 ± 0.09 μ m) and YM (1.81 ± 0.17 μ m, Figure 3A). Type II SC niche laminin thickness was significantly greater in OM (1.86 ± 0.06 μ m) as compared to YM (1.55 ± 0.09 μ m, $p < 0.05$, Figure 3A). The percentage of type I-associated SC that were incarcerated by

laminin was significantly greater in OM ($28.4 \pm 8.2\%$) as compared to YM ($3.6 \pm 2.1\%$; $p < 0.05$). The percentage of type II-associated SC that were incarcerated by laminin was significantly greater in OM ($13.6 \pm 4.2\%$) as compared to YM ($3.5 \pm 1.5\%$; $p < 0.05$). We also observed that in the basal state, 100% of OM participants had evidence of at least one incarcerated SC, compared to ~40% of YM participants. After making this observation, we continued with additional experiments to determine whether these incarcerated SC responded differently to acute exercise or adapted to chronic exercise training.

SC nuclei measurements: In mixed fibre type muscle, SC DAPI+ nuclear CSA was significantly greater in OM ($17.94 \pm 0.79 \mu\text{m}^2$) as compared to YM ($15.28 \pm 0.42 \mu\text{m}^2$, $p < 0.05$). The relative area that was covered by the SC nucleus (i.e., DAPI+ nuclear signature) within the niche percentage was not significantly different between OM ($70.7 \pm 1.4 \%$) and YM ($67.6 \pm 1.2 \%$). When assessed by fibre-type, type I SC DAPI+ nuclear CSA was not significantly different ($p = 0.08$) between OM ($18.44 \pm 1.05 \mu\text{m}^2$) and YM ($15.05 \pm 1.42 \mu\text{m}^2$). Type II SC DAPI+ nuclear CSA was significantly greater in OM ($16.03 \pm 1.15 \mu\text{m}^2$) as compared to the YM group ($12.74 \pm 0.69 \mu\text{m}^2$, $p < 0.05$, Figure 3B).

Alterations of the muscle following 12-weeks of a combined exercise training program in healthy older men (OM-Ex)

Indices of fibrosis and collagen composition in mixed fibre type muscle following training: Prior to exercise training, the fibrotic index as measured by Masson's trichrome staining was $6.1 \pm 0.8\%$ and was not significantly changed following training ($6.7 \pm 0.8\%$) in OM. **Similarly, there was no change in collagen IV pre- ($14.2 \pm 0.9\%$) as compared to post-training program ($17.5 \pm 1.1\%$, $p > 0.05$). Following training, there was a significant increase in collagen VI content ($17.2 \pm 1.0\%$), as compared to pre-training ($15.6 \pm 1.0\%$, $p < 0.05$). In contrast, there was a non-significant ($p = 0.07$) decrease in laminin content following training ($13.3\% \pm 0.6$), as compared to pre- exercise training ($15.5 \pm 0.8 \%$) in OM.**

Determining whether the proportion of SC incarceration changes with acute exercise. During the PRE-trained condition, prior to the acute bout of resistance exercise in the OM-Ex (Pre), we observed that the proportion of total SC that were incarcerated was $16.4 \pm 2.3\%$. The proportion of total SC that were incarcerated remained unchanged at 24h- or 48h-post exercise recovery

($26.5 \pm 2.7\%$, $21.3 \pm 2.7\%$ respectively, Figure 4). During the POST condition, prior to the acute bout of resistance exercise in the OM-Ex (Pre), we observed that the proportion of total SC that were incarcerated was $12.4 \pm 1.6\%$. The proportion of total SC that were incarcerated was not changed at 24h- or 48h-post exercise recovery ($14.9 \pm 1.9\%$, $21.2 \pm 3.4\%$, respectively, $p > 0.05$ Figure 4). The mean incarceration proportion is significantly lowered in POST compared to PRE but does not significantly change with within the first 48h following a single bout of resistance exercise.

Determining whether chronic exercise training alters SC incarceration proportion. Prior to the 12 wks of exercise training, we observed that mean SC incarceration (representative of the proportion of total SC incarceration, which included quiescent and active SC) was $21.6 \pm 1.8\%$. Following chronic training, the mean SC incarceration was significantly lower $15.8\% \pm 1.5$ ($p < 0.05$). Due to the fact that there were no observable changes in SC incarceration proportion in response to an acute bout of exercise, the mean incarceration proportion was calculated by averaging the proportion of total SC incarceration across the Pre-, 24h-post and 48h-post exercise time points.

SC incarceration in response to a single bout of exercise. In the PRE-chronic training condition, prior to the acute bout of resistance exercise in OM-Ex group (Pre), observed that within the population of activated SC (Pax7+/MyoD+), $94.7 \pm 2.6\%$ of activated SC were not incarcerated, compared with $5.3 \pm 2.6\%$ ($p < 0.05$) of active incarcerated SC. Following 24h- and 48h-post exercise recovery, this remained unchanged, with the percentage of activated SC ($91.9 \pm 2.8\%$, $90.3 \pm 3.1\%$, respectively) that were not incarcerated remaining significantly greater ($p < 0.05$) than the those that were incarcerated ($8.1 \pm 2.8\%$, $9.7\% \pm 3.1\%$, respectively, Figure 5A). Similarly, during the bout of exercise POST-training, the proportion of activated SC was significantly greater in the non-incarcerated condition in the Pre-, 24h- and 48h-post exercise ($96.4 \pm 1.5\%$, $95.8 \pm 1.8\%$, $95.3 \pm 1.9\%$, respectively) as compared to the incarcerated condition ($3.6 \pm 1.5\%$, $4.2 \pm 1.8\%$, $4.7 \pm 1.9\%$, respectively, Figure 5B)

Proportion of active and quiescent incarcerated SC. In the PRE-chronic training condition, prior to the acute bout of resistance exercise in OM-Ex group (Pre), there was a significantly greater number of active SC in the non-incarcerated as compared to the incarcerated condition ($21.5 \pm 3.5\%$ vs. $8.2 \pm 4.9\%$, respectively, $p < 0.05$, Figure 6A). Following 24h, there was still a

significantly greater number of active SC in the non-incarcerated as compared to the incarcerated condition ($26.0 \pm 4.7\%$ vs. $8.4 \pm 3.3\%$, respectively, $p < 0.05$, Figure 6A). At 48h post-exercise, the proportion of activation between non-incarcerated as compared to incarcerated SC remained different ($31.7 \pm 4.7\%$ vs. $32.0 \pm 8.7\%$, respectively, $p < 0.05$). Similarly, in the POST condition, there was a significantly greater number of non-incarcerated active SC at Pre-exercise, and 48h-post exercise ($24.3 \pm 4.2\%$, $30.8 \pm 4.6\%$ respectively) as compared to incarcerated active SC at the same timepoints ($7.2 \pm 3.3\%$, $15.2 \pm 5.9\%$ respectively, $p < 0.05$, Figure 6B). In order to determine whether alterations to the biophysical thickness of the laminin and/or the incarceration of the laminin, we performed *in vitro* transwell migration assay using C2C12 myoblasts. Fewer cells were able to migrate through the transwell when a concentration of 400 or 800 $\mu\text{g/mL}$ of Matrigel was used compared to a concentration of 200 $\mu\text{g/mL}$. No differences existed in the number of migrated cells when a concentration of 400 or 800 $\mu\text{g/mL}$ of Matrigel was used.

Determining whether SC incarceration is associated with gross measures of leg lean mass. We correlated the PRE- to POST-training mean incarceration proportion change with the change in DEXA lean leg mass ($p < 0.05$, $r = -0.43$, Figure 7). We found that the change in mean incarceration proportion was not correlated to the change in leg strength as assessed by the Σ lower body exercises (kg) ($p > 0.05$, $r = 0.15$).

DISCUSSION:

We report a thicker laminin surrounding of the SC niche in OM as compared to YM. To the best of our knowledge, we are the first to describe and quantify, via confocal microscopy, that there is an extensive increased localization of laminin in the SC niche, in some cases incarcerating SC in OM. Following acute resistance exercise in older men, incarcerated SC were less likely to become activated (MyoD⁺Pax7⁺). Further, we report that the number of incarcerated SC was lower following 12-wks of exercise training, and that this change is associated with greater gains in leg lean mass. Finally, we report that there was a marked difference in the composition of the ECM in OM, with increases in general fibrosis, laminin protein content and lower collagen IV protein content in OM as compared to YM.

Skeletal muscle aging is characterized by a reduction in type II muscle fibre size (Lexell *et al.*, 1988; Verdijk *et al.*, 2007; Nilwik *et al.*, 2013), collagen infiltration and an alteration in

the muscle ECM (Kragstrup *et al.*, 2011; Thomas *et al.*, 2015; Garg & Boppart, 2016). These changes, including infiltration of non-contractile material, ultimately reduce muscle quality (Ryall *et al.*, 2008). As skeletal muscle SC have been proposed to play a crucial role in muscle fibre maintenance and remodeling, a reduction in SC number and/or function may be a critical factor in the development of type II muscle fibre atrophy with aging (Kadi *et al.*, 2004; Verdijk *et al.*, 2007), but also the development of muscle fibrosis (Brack *et al.*, 2007). The data in the present study suggests a thickening of the basal lamina associated with type II SC with aging. Work by Brack and colleagues (2007) suggests that a loss of SC may reduce muscle quality and may contribute to increased fibrosis observed in aged muscle. Interestingly, the relationship between fibrosis and SC content may be exacerbated in type II muscle fibres, as evidence suggests that SC limit fibrosis preferentially in type II muscle fibres (Morrison *et al.*, 2000; Fry *et al.*, 2015). We propose that the loss of type II muscle fibre SC content typically observed with aging may propagate an increase in fibrosis resulting in thicker laminin in type II muscle fibres as compared to YM as observed in the present study.

In older adults, SC have previously been shown to have a blunted activation and proliferation response to exercise (McKay *et al.*, 2012; Snijders *et al.*, 2014). In OM, we report that a greater number of SC are fully incarcerated by laminin as compared to their younger counterparts. We also report that incarcerated SC in OM are less likely to become active (MyoD⁺/Pax7⁺) following a bout of resistance exercise. Following 12 weeks of an exercise training program that combined resistance exercise training and high-intensity interval exercise training, we observed a significant reduction in the proportion of SC that were incarcerated. While it was not measured in the present study, a recent publication by Snijders and colleagues using the same subjects (Snijders *et al.*, 2019) have shown that following exercise training, there was an enhanced activation of muscle SC following an acute bout of resistance exercise. We were unable to observe whether individual incarcerated SC become activated following exercise; however, our findings suggest that the resistance exercise stimulus that was sufficient in stimulating other, non-incarcerated SC into activation. As a component of the SC niche, the muscle ECM serves as structural support (Kragstrup *et al.*, 2011) and propagates external signaling molecules through the niche (Harburger & Calderwood, 2009). There are numerous circulating growth factors that have been implicated in the activation and/or expansion of the SC pool (e.g., IGF-1, IL-6, Myostatin, HGF) (Snijders *et al.*, 2015). An exaggerated laminin

deposition and infiltration of the SC niche may act as a physical barrier for systemic growth/signaling factors to move across the basal lamina and interact with the SC. Greater laminin infiltration (i.e., incarceration) may also impact SC responsiveness and function by reducing growth factor signal from sources internal and/or external to the myofibre. We hypothesize that the greater levels of incarcerated SC in OM observed in the present study may therefore reduce the physical interaction of SC with the other muscle resident structures and/or cell populations (Labat-Robert, 2003). Furthermore, thickening of laminin associated with the SC niche may also contribute to increased ECM stiffness, which is known to reduce the proliferative ability of the SC (Lacraz *et al.*, 2015; Trenszt *et al.*, 2015). Consistent with this notion, we observe that non-incarcerated SC make up approximately 90% of all activated MyoD⁺/Pax7⁺ cells in both a basal state or following a bout of resistance exercise in OM-Ex. Taken together, we propose that greater laminin infiltration and incarceration of SC may play an important role in the blunting of SC activation following resistance exercise in older adults. However, the level of incarceration observed in OM can be ameliorated by long-term exercise training, suggesting connective tissue remodeling, which occurs concomitantly with enhanced muscle SC activation.

Changes in ECM protein composition may also impact SC function and/or content. An increase in collagen content (Kovanen *et al.*, 1987; Ramaswamy *et al.*, 2011) and collagen concentration (Alnaqeeb *et al.*, 1984) has repeatedly been reported in skeletal muscle with age. Similarly, we report significantly greater overall collagen content in OM as compared to YM, based on masson trichrome staining. Following 12-wks of the combined exercise training program in OM-Ex, there did not appear to be any significant change in overall fibrosis. However, there are multiple isoforms of collagen with various functional characteristics (Kjaer, 2004), and aging appears to specifically increase levels of some subtypes while decreasing others (Hindle *et al.*, 2009). We observed that collagen type IV protein content, an integral part of the basement membrane alongside laminin (Sanes, 2003) appears to be significantly lower in older adults as compared to their young counterparts. While there is limited data in humans, work in rats supports this finding, as there is a marked reduction in the ratio of type IV collagen to laminin, especially in fast twitch muscle fibres (Kovanen *et al.*, 1988). In humans, our observation that there is a decreased collagen IV muscle content in aged individuals is in keeping with previous literature from aging human skin samples (Feru *et al.*, n.d.; Vázquez *et al.*, 1996).

Interestingly, we observe that not only was there a marked thickening of the basal lamina surrounding SC in OM as compared to YM, there was also a greater overall expression of laminin in muscle. However, following 12 wks of exercise training, there was a trend for a lower laminin expression ($p = 0.07$) in OM-Ex, suggesting that exercise training resulted in remodeling and may lead to a reduction in laminin with aging. We did not observe any change in collagen IV with 12-wks of exercise training in OM-Ex, We did not observe any age related alteration in protein content of collagen V and VI. Recent work suggests that collagen VI is an important aspect of the SC niche (Urciuolo *et al.*, 2013) and is critical for the self-renewal capacity of SC (Urciuolo *et al.*, 2013). Considering implications for mutations in collagen VI genes in humans (i.e., myopathy, dystrophy) (Lampe & Bushby, 2005), and that collagen VI-null mice exhibit extensively impaired muscle regeneration (Urciuolo *et al.*, 2013). Although in our hands collagen VI was not altered by aging at the whole muscle level there may have been alterations that occurred directly within the niche itself, however we were unable to assess this in the current investigation. increase collagen VI expression with chronic exercise training may be beneficial to the resident muscle SC in older muscle. Collectively, these data suggest that there are age-related changes in the ECM composition, which can be “corrected” with chronic exercise training.

The alterations of the ECM and increased fibrosis may be associated with a change in SC nuclear size. Interestingly, we observe that type II muscle fibre SC Pax7+/DAPI+ nuclear CSA was significantly greater (~30%) in OM as compared to YM. While we were not able to calculate total volume of the DAPI+ nuclear (and instead used nuclear CSA as a proxy), and we understand that the 2D nature of using cryosections to assess area is limited, we took into account ~350 individual SC via high resolution confocal microscopy, which to our knowledge is the first time this measurement has been made in human tissue. An increase in nuclear size is characteristic of transcriptional activity (Marguerat & Bahler, 2012), it may also indicate cellular senescence (Mitsui & Schneider, 1976; Sadaie *et al.*, 2015). Evidence suggests that p16^{INK4a}, a marker of cellular senescence (Stein *et al.*, 1999), has been observed in aged SC (Sousa-Victor *et al.*, 2014; Garcia-Prat *et al.*, 2016). Due to technical limitations, we were not able to co-stain p16^{INK4a} and Pax7+/DAPI+ cells. However, work by Carlson and colleagues (Carlson *et al.*, 2008) suggests that signaling from the aged SC niche may upregulate p16. Therefore, it stands to reason that the observed increase in nuclear size of SC in OM may be reflective of an upregulation of p16 and entry of a greater proportion of the SC pool into senescence. We

speculate that this enlargement of type II muscle fibre SC in OM may therefore be related to thickening and altered composition of the ECM.

The processes governing ECM synthesis and breakdown may also be modified by aging. Senescent cells, often associated with aging, can also alter the ECM through alterations in collagen and laminin chains (Liu & Hornsby, 2007; Sprenger *et al.*, 2008). By measuring the mRNA of various collagen subtypes and laminin chains in human muscle (i.e, subtypes apparent in laminin-211), we observed that there was an overall greater expression in aging as compared to young individuals. We observe that there is an increased mRNA expression in laminin subunits, concomitant with a greater laminin protein content, laminin thickness as measured at the niche, and laminin infiltration (i.e., incarceration) in aged individuals. Interestingly, we also observed an overall decrease in protein expression of collagen IV in OM as compared to YM, despite no changes in mRNA expression. We speculate that while the mRNA expression for collagen IV is unchanged in OM, there may be a disconnect between transcription and translation in protein. These findings may also be explained by a greater breakdown of collagen IV via enzymatic processes. Consistent with this notion, we observed that mRNA expression of matrix metalloproteinase-2 (MMP-2), an enzyme responsible for the breakdown for type IV collagen and laminin (Lu *et al.*, 2011), was significantly greater in OM as compared to YM. It is possible that the relationship between synthesis of collagen IV and the enzymatic breakdown via MMP-2 becomes dysregulated with age. The increase in MMP-2 expression may also be in response to increases in laminin in OM. While we did not measure the localization of MMP-2, previous work suggests that intracellular MMP-2 expression occurs to a large extent in type II fibres, suggesting that ECM remodelling may be more pronounced in type II fibres (Hadler-Olsen *et al.*, 2015). Considering that we observe a thickening of laminin primarily associated with the type II muscle fibres, we speculate that the elevated expression of MMP-2 may be an attempt to facilitate normal ECM turnover and/or maintenance. Future studies should aim to address the 3D nature of the SC niche, namely whether or not the thickening of the lamina or the incarceration that we observe in aging is consistent throughout the entirety of the SC niche.

The findings of the present study suggest that there is thickening of laminin around SC specifically associated with type II muscle fibres, concomitant with an increased SC incarceration in OM as compared to YM. Previously, we and others observed reduced type II

muscle fibre-associated SC content (Verdijk *et al.*, 2007) as well as delayed type II muscle fibre SC expansion following a single exercise bout (McKay *et al.*, 2012; Snijders *et al.*, 2014; Nederveen *et al.*, 2015). The reduction in content and diminished responsiveness of SC in aged type II muscle fibres may stem from the changes in the muscle ECM observed here, as it has been shown repeatedly that negative alterations in the SC niche results in reduced regenerative capacity across nearly all stem cell populations (Jones & Wagers, 2008). With chronic exercise training, there are beneficial alterations to the SC niche, including a reduction in SC incarceration. Recently published work using the same tissue has shown that following training, there is an enhanced activation of muscle SC (Snijders *et al.*, 2019). Whether the observed increase is basal lamina thickness or incarceration of the muscle SC has direct implications on the ability for SC to become activated following stimuli remains to be fully elucidated. Future studies should address whether the incarcerated SC observed in this study express markers for cellular senescence, an inability to become activated following stimuli such as exercise, or whether the changes in fibrosis or the SC niche can be rejuvenated with chronic exercise.

We conclude that the structural properties of the SC niche are altered by age. The greater thickness and incarceration of SC by laminin as well as reduction in collagen IV content observed in OM, may be an important factor in the impaired regulation of the SC pool in aged muscle.

ACKNOWLEDGEMENTS

The Pax7 hybridoma cells developed by Dr.A. Kawakami, the A4.951 developed by Dr. H. Blau were obtained from the Developmental Studies Hybridoma Bank, created by the NICHD of the NIH and maintained at The University of Iowa, Department of Biology, Iowa City, IA 52242. Dr. G Parise was supported by a Natural Sciences and Engineering Research Council of Canada (NSERC) Grant (1455843), JP Nederveen by a NSERC Canadian Graduate Scholarship (CGS-D). There are no conflict of interests.

AUTHOR CONTRIBUTIONS

J.P Nederveen, T Snijders, K.E. Bell, S.M. Phillips and G. Parise conceived and designed research; J.P Nederveen, T Snijders, K.E. Bell, S Joannis, D. Kumbhare collected the tissue; J.P Nederveen, T Snijders, A.C.Q. Thomas analyzed data; J.P Nederveen, A.C.Q Thomas, T

Snijders, S Joannisse, K.E. Bell, S.M. Phillips, D. Kumbhare and G. Parise interpreted results; J.P Nederveen, A.C.Q Thomas prepared figures; J.P Nederveen drafted the manuscript; J.P Nederveen, A.C.Q Thomas, T Snijders, S Joannisse, K.E. Bell, S.M. Phillips, D. Kumbhare and G Parise edited and revised manuscript; J.P Nederveen, A.C.Q Thomas, T Snijders, S Joannisse, K.E. Bell, S.M. Phillips, D. Kumbhare and G Parise approved final version of the manuscript.

FIGURE CAPTIONS

Figure 1. Representative image of an incarcerated satellite cell within a muscle cross section. (A) channel views of a merged image (B) Laminin (C) Pax7/Laminin (D) Laminin/DAPI (E) Pax7/DAPI. Representative image of a non-incarcerated satellite cell within a muscle cross section, for comparison. (F) channel views of a merged image (G) Laminin (H) Pax7/Laminin (I) Laminin/DAPI (J) Pax7/DAPI.

Figure 2. Representation of altered fibrotic tissue content in skeletal muscle with aging. Masson's Trichrome staining was performed on tissue from young (A) and old (B) men. More collagen positive area (tissue stained blue) was found in the skeletal muscle of aged individuals (C). *Significantly different compared with young men (YM) ($p < 0.05$). Values are reported as a percentage, mean \pm SEM.

Figure 3. Representative western blot of laminin, collagen VI, collagen V and collagen VI in *vastus lateralis* muscles of young (YM) and old (OM) men. A Ponceau S stain is displayed below each protein of interest to indicate equal loading between samples. *Significantly different compared with young men (YM) ($p < 0.05$). Values are reported as arbitrary units, mean \pm SEM.

Figure 4. Representation of mRNA gene expression of various collagen components (COL1 α 1, COL3 α 1, COL4 α 1, COL6 α 1), type IV collagenase (matrix metalloproteinase-2. MMP-2), and various laminin components (LAM α 2, LAM β 1, LAM γ 1). Data are normalized to GAPDH. *Significantly different compared with young men (YM) ($p < 0.05$). Values are reported as arbitrary units, mean \pm SEM.

Figure 5. Anatomical descriptions of the satellite cell niche. Representation of (A) basal lamina thickness (μm) in a fibre type specific manner (B) nuclear cross-sectional area (μm^2) in young and old men. *Significantly different compared with young men (YM) ($p < 0.05$).

Figure 6. The percentage of satellite cells (SC) that are incarcerated is reduced after a 12-week a combined exercise training program in old men, with no effect of time. *Significantly different compared with pre-training condition ($p < 0.05$). Values are reported as mean \pm SEM.

Figure 7. Incarcerated satellite cells (SC) are less activated than their non-incarcerated counterparts following an acute bout of exercise. Representation of the percentage of activated satellite cells (Pax7⁺/MyoD⁺) that are incarcerated during an acute bout of exercise (A) prior to (B) following 12 wks of a combined exercise training program. *Significantly different compared with pre-training condition ($p < 0.05$). Values are reported as mean \pm SEM.

Figure 8. Proportion of satellite cell subpopulations that were incarcerated or non-incarcerated during the response to a bout of exercise prior to (A) and following (B) 12 wks of a combined exercise training program. *Significantly different from non-incarcerated SC within the timepoint shown. Representative image of a quiescent (MyoD⁻/Pax7⁺) and activated (MyoD⁺/Pax7⁺) satellite cell within the skeletal muscle of an aged male. (C) channel views of a merged image (D) Pax7/DAPI and (E) MyoD/DAPI.

Figure 9. The relationship between the change in DEXA-derived lean leg mass and the change in incarcerated SC proportion ($p < 0.05$, $r = -0.43$) following 12 weeks of a combined exercise training program.

REFERENCES

- Alnaqeeb MA, Al Zaid NS & Goldspink G (1984). Connective tissue changes and physical properties of developing and ageing skeletal muscle. *J Anat* **139** (Pt 4, 677–689).
- Bell KE, Snijders T, Zulyniak M, Kumbhare D, Parise G, Chabowski A & Phillips SM (2017). A whey protein-based multi-ingredient nutritional supplement stimulates gains in lean body mass and strength in healthy older men: A randomized controlled trial. *PLoS One* **12**,

e0181387.

- Bentzinger CF, Wang YX, Dumont NA & Rudnicki MA (2013). Cellular dynamics in the muscle satellite cell niche. *EMBO Rep* **14**, 1062–1072.
- Brack AS, Conboy MJ, Roy S, Lee M, Kuo CJ, Keller C & Rando TA (2007). Increased Wnt signaling during aging alters muscle stem cell fate and increases fibrosis. *Science (80-)* **317**, 807–810.
- Candiello J, Cole GJ & Halfter W (2010). Age-dependent changes in the structure, composition and biophysical properties of a human basement membrane. *Matrix Biol* **29**, 402–410.
- Carlson ME, Hsu M & Conboy IM (2008). Imbalance between pSmad3 and Notch induces CDK inhibitors in old muscle stem cells. *Nature* **454**, 528–532.
- Christov C, Chretien F, Abou-Khalil R, Bassez G, Vallet G, Authier FJ, Bassaglia Y, Shinin V, Tajbakhsh S, Chazaud B & Gherardi RK (2007). Muscle satellite cells and endothelial cells: close neighbors and privileged partners. *Mol Biol Cell* **18**, 1397–1409.
- Feru J, Delobbe E, Ramont L, Brassart B, Terryn C, Dupont-Deshorgue A, Garbar C, Monboisse J-C, Maquart F-X & Brassart-Pasco S (n.d.). Aging decreases collagen IV expression in vivo in the dermo-epidermal junction and in vitro in dermal fibroblasts: possible involvement of TGF- β 1. *Eur J Dermatology* **26**, 350–360.
- Fry CS, Lee JD, Mula J, Kirby TJ, Jackson JR, Liu F, Yang L, Mendias CL, Dupont-Versteegden EE, McCarthy JJ & Peterson CA (2015). Inducible depletion of satellite cells in adult, sedentary mice impairs muscle regenerative capacity without affecting sarcopenia. *Nat Med* **21**, 76–80.
- Garcia-Prat L, Martinez-Vicente M, Perdiguero E, Ortet L, Rodriguez-Ubreva J, Rebollo E, Ruiz-Bonilla V, Gutarra S, Ballestar E, Serrano AL, Sandri M & Munoz-Canoves P (2016). Autophagy maintains stemness by preventing senescence. *Nature* **529**, 37–42.
- Garg K & Boppart MD (2016). Influence of exercise and aging on extracellular matrix composition in the skeletal muscle stem cell niche. *J Appl Physiol* **121**, 1053–1058.
- Hadler-Olsen E, Solli AI, Hafstad A, Winberg JO & Uhlin-Hansen L (2015). Intracellular MMP-2 activity in skeletal muscle is associated with type II fibers. *J Cell Physiol* **230**, 160–169.
- Harburger DS & Calderwood DA (2009). Integrin signalling at a glance. *J Cell Sci* **122**, 159–163.
- Hindle AG, Horning M, Mellish JA & Lawler JM (2009). Diving into old age: muscular senescence in a large-bodied, long-lived mammal, the Weddell seal (*Leptonychotes weddellii*). *J Exp Biol* **212**, 790–796.
- Joe AW, Yi L, Natarajan A, Le Grand F, So L, Wang J, Rudnicki MA & Rossi FM (2010). Muscle injury activates resident fibro/adipogenic progenitors that facilitate myogenesis. *Nat Cell Biol* **12**, 153–163.

- Jones DL & Wagers AJ (2008). No place like home: anatomy and function of the stem cell niche. *Nat Rev Mol Cell Biol* **9**, 11–21.
- Kadi F, Charifi N, Denis C & Lexell J (2004). Satellite cells and myonuclei in young and elderly women and men. *Muscle Nerve* **29**, 120–127.
- Kjaer M (2004). Role of extracellular matrix in adaptation of tendon and skeletal muscle to mechanical loading. *Physiol Rev* **84**, 649–698.
- Kovanen V, Suominen H & Peltonen L (1987). Effects of aging and life-long physical training on collagen in slow and fast skeletal muscle in rats. A morphometric and immunohistochemical study. *Cell Tissue Res* **248**, 247–255.
- Kovanen V, Suominen H, Risteli J & Risteli L (1988). Type IV collagen and laminin in slow and fast skeletal muscle in rats--effects of age and life-time endurance training. *Coll Relat Res* **8**, 145–153.
- Kragstrup TW, Kjaer M & Mackey AL (2011). Structural, biochemical, cellular, and functional changes in skeletal muscle extracellular matrix with aging. *Scand J Med Sci Sport* **21**, 749–757.
- Labat-Robert J (2003). Age-dependent remodeling of connective tissue: role of fibronectin and laminin. *Pathol Biol* **51**, 563–568.
- Lacraz G, Rouleau AJ, Couture V, Sollrard T, Drouin G, Veillette N, Grandbois M & Grenier G (2015). Increased Stiffness in Aged Skeletal Muscle Impairs Muscle Progenitor Cell Proliferative Activity. *PLoS One* **10**, e0136217.
- Lampe AK & Bushby KMD (2005). Collagen VI related muscle disorders. *J Med Genet* **42**, 673–685.
- Lepper C, Partridge TA & Fan CM (2011). An absolute requirement for Pax7-positive satellite cells in acute injury-induced skeletal muscle regeneration. *Development* **138**, 3639–3646.
- Lexell J, Taylor CC & Sjoström M (1988). What is the cause of the ageing atrophy? Total number, size and proportion of different fiber types studied in whole vastus lateralis muscle from 15- to 83-year-old men. *J Neurol Sci* **84**, 275–294.
- Liu D & Hornsby PJ (2007). Senescent Human Fibroblasts Increase the Early Growth of Xenograft Tumors via Matrix Metalloproteinase Secretion. *Cancer Res* **67**, 3117–3126.
- Lu P, Takai K, Weaver VM & Werb Z (2011). Extracellular matrix degradation and remodeling in development and disease. *Cold Spring Harb Perspect Biol*; DOI: 10.1101/cshperspect.a005058.
- Marguerat S & Bahler J (2012). Coordinating genome expression with cell size. *Trends Genet* **28**, 560–565.
- Mauro A (1961). Satellite cell of skeletal muscle fibers. *J Biophys Biochem Cytol* **9**, 493–495.
- McCarthy JJ, Mula J, Miyazaki M, Erfani R, Garrison K, Farooqui AB, Srikuea R, Lawson BA,

- Grimes B, Keller C, Van Zant G, Campbell KS, Esser KA, Dupont-Versteegden EE & Peterson CA (2011). Effective fiber hypertrophy in satellite cell-depleted skeletal muscle. *Development* **138**, 3657–3666.
- McCarthy RA & Hay ED (1991). Collagen I, laminin, and tenascin: ultrastructure and correlation with avian neural crest formation. *Int J Dev Biol* **35**, 437–452.
- McKay BR, Ogborn DI, Bellamy LM, Tarnopolsky MA & Parise G (2012). Myostatin is associated with age-related human muscle stem cell dysfunction. *FASEB J* **26**, 2509–2521.
- Mitsui Y & Schneider EL (1976). Increased nuclear sizes in senescent human diploid fibroblast cultures. *Exp Cell Res* **100**, 147–152.
- Morrison J, Lu QL, Pastoret C, Partridge T & Bou-Gharios G (2000). T-cell-dependent fibrosis in the mdx dystrophic mouse. *Lab Invest* **80**, 881–891.
- Nederveen JP, Joanisse S, Séguin CML, Bell KE, Baker SK, Phillips SM & Parise G (2015). The effect of exercise mode on the acute response of satellite cells in old men. *Acta Physiol*; DOI: 10.1111/apha.12601.
- Nederveen JP, Joanisse S, Snijders T, Ivankovic V, Baker SK, Phillips SM & Parise G (2016). Skeletal muscle satellite cells are located at a closer proximity to capillaries in healthy young compared with older men. *J Cachexia Sarcopenia Muscle*; DOI: 10.1002/jcsm.12105.
- Nederveen JP, Joanisse S, Snijders T, Thomas ACQ, Kumbhare D & Parise G (2018). The influence of capillarization on satellite cell pool expansion and activation following exercise-induced muscle damage in healthy young men. *J Physiol*; DOI: 10.1113/JP275155.
- Nilwik R, Snijders T, Leenders M, Groen BB, van Kranenburg J, Verdijk LB & van Loon LJ (2013). The decline in skeletal muscle mass with aging is mainly attributed to a reduction in type II muscle fiber size. *Exp Gerontol* **48**, 492–498.
- Pedersen BK & Febbraio MA (2008). Muscle as an endocrine organ: focus on muscle-derived interleukin-6. *Physiol Rev* **88**, 1379–1406.
- Ramaswamy KS, Palmer ML, van der Meulen JH, Renoux A, Kostrominova TY, Michele DE & Faulkner JA (2011). Lateral transmission of force is impaired in skeletal muscles of dystrophic mice and very old rats. *J Physiol* **589**, 1195–1208.
- Ryall JG, Schertzer JD & Lynch GS (2008). Cellular and molecular mechanisms underlying age-related skeletal muscle wasting and weakness. *Biogerontology* **9**, 213–228.
- Sadaie M, Dillon C, Narita M, Young AR, Cairney CJ, Godwin LS, Torrance CJ, Bennett DC, Keith WN & Narita M (2015). Cell-based screen for altered nuclear phenotypes reveals senescence progression in polyploid cells after Aurora kinase B inhibition. *Mol Biol Cell* **26**, 2971–2985.
- Sambasivan R, Yao R, Kissenpfennig A, Van Wittenberghe L, Paldi A, Gayraud-Morel B, Guenou H, Malissen B, Tajbakhsh S & Galy A (2011). Pax7-expressing satellite cells are

- indispensable for adult skeletal muscle regeneration. *Development* **138**, 3647–3656.
- Sanes JR (2003). The basement membrane/basal lamina of skeletal muscle. *J Biol Chem* **278**, 12601–12604.
- Schmittgen TD & Livak KJ (2008). Analyzing real-time PCR data by the comparative C(T) method. *Nat Protoc* **3**, 1101–1108.
- Snijders T, Nederveen JP, Bell KE, Lau SW, Mazara N, Kumbhare DA, Phillips SM & Parise G (2019). Prolonged exercise training improves the acute type II muscle fibre satellite cell response in healthy older men. *J Physiol* **597**, 105–119.
- Snijders T, Nederveen JP, McKay BR, Joannis S, Verdijk LB, van Loon LJC & Parise G (2015). Satellite cells in human skeletal muscle plasticity. *Front Physiol*; DOI: 10.3389/fphys.2015.00283.
- Snijders T, Verdijk LB, Smeets JS, McKay BR, Senden JM, Hartgens F, Parise G, Greenhaff P & van Loon LJ (2014). The skeletal muscle satellite cell response to a single bout of resistance-type exercise is delayed with aging in men. *Age* **36**, 9699.
- Snow MH (1977). The effects of aging on satellite cells in skeletal muscles of mice and rats. *Cell Tissue Res* **185**, 399–408.
- Sousa-Victor P, Gutarra S, Garcia-Prat L, Rodriguez-Ubreva J, Ortet L, Ruiz-Bonilla V, Jordi M, Ballestar E, Gonzalez S, Serrano AL, Perdiguero E & Munoz-Canoves P (2014). Geriatric muscle stem cells switch reversible quiescence into senescence. *Nature* **506**, 316–321.
- Sprenger CCT, Drivdahl RH, Woodke LB, Eyman D, Reed MJ, Carter WG & Plymate SR (2008). Senescence-induced alterations of laminin chain expression modulate tumorigenicity of prostate cancer cells. *Neoplasia* **10**, 1350–1361.
- Stein GH, Drullinger LF, Soulard A & Dulic V (1999). Differential roles for cyclin-dependent kinase inhibitors p21 and p16 in the mechanisms of senescence and differentiation in human fibroblasts. *Mol Cell Biol* **19**, 2109–2117.
- Thomas K, Engler AJ & Meyer GA (2015). Extracellular matrix regulation in the muscle satellite cell niche. *Connect Tissue Res* **56**, 1–8.
- Trensz F, Lucien F, Couture V, Sollrard T, Drouin G, Rouleau AJ, Grandbois M, Lacraz G & Grenier G (2015). Increased microenvironment stiffness in damaged myofibers promotes myogenic progenitor cell proliferation. *Skelet Muscle* **5**, 5.
- Urciuolo A, Quarta M, Morbidoni V, Gattazzo F, Molon S, Grumati P, Montemurro F, Tedesco FS, Blaauw B, Cossu G, Vozzi G, Rando TA & Bonaldo P (2013). Collagen VI regulates satellite cell self-renewal and muscle regeneration. *Nat Commun* **4**, 1964.
- Vázquez F, Palacios S, Alemañ N & Guerrero F (1996). Changes of the basement membrane and type IV collagen in human skin during aging. *Maturitas* **25**, 209–215.
- Verdijk LB, Koopman R, Schaart G, Meijer K, Savelberg HH & van Loon LJ (2007). Satellite

cell content is specifically reduced in type II skeletal muscle fibers in the elderly. *Am J Physiol Endocrinol Metab* **292**, E151-7.

Verdijk LB, Snijders T, Drost M, Delhaas T, Kadi F & van Loon LJ (2014). Satellite cells in human skeletal muscle; from birth to old age. *Age* **36**, 545–547.

Figure 1

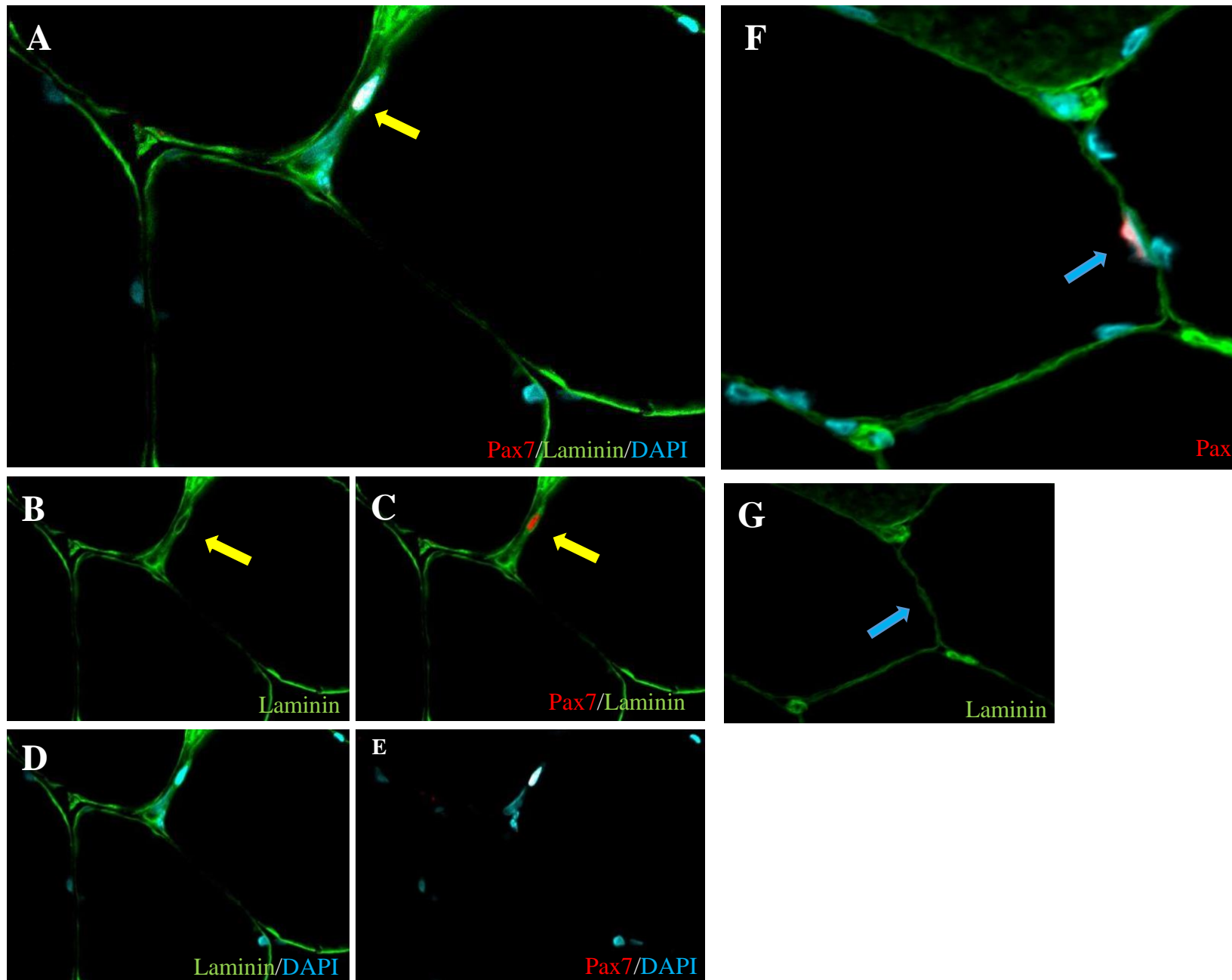
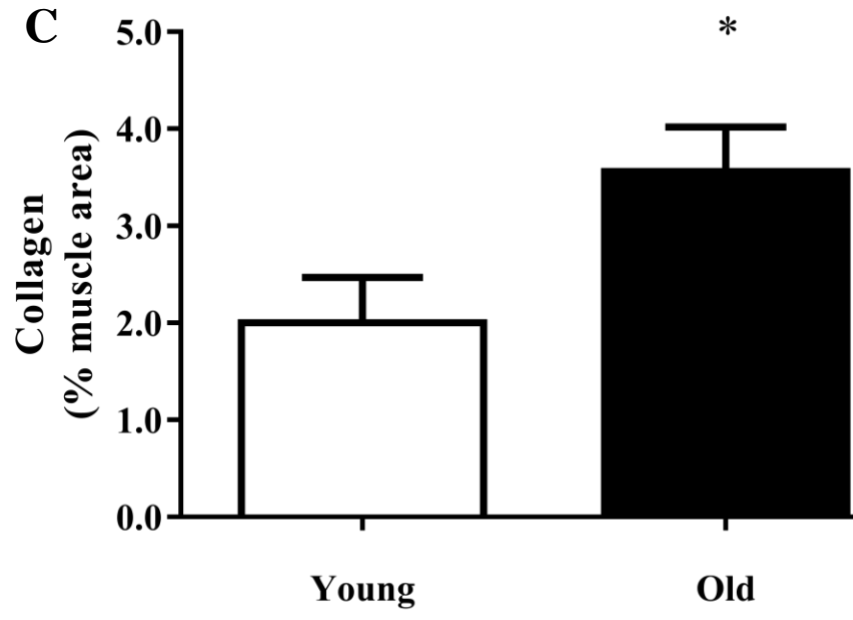
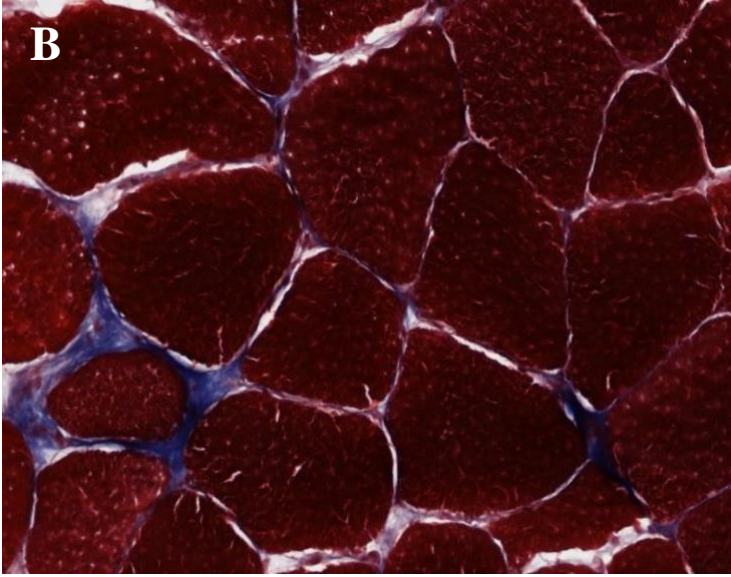
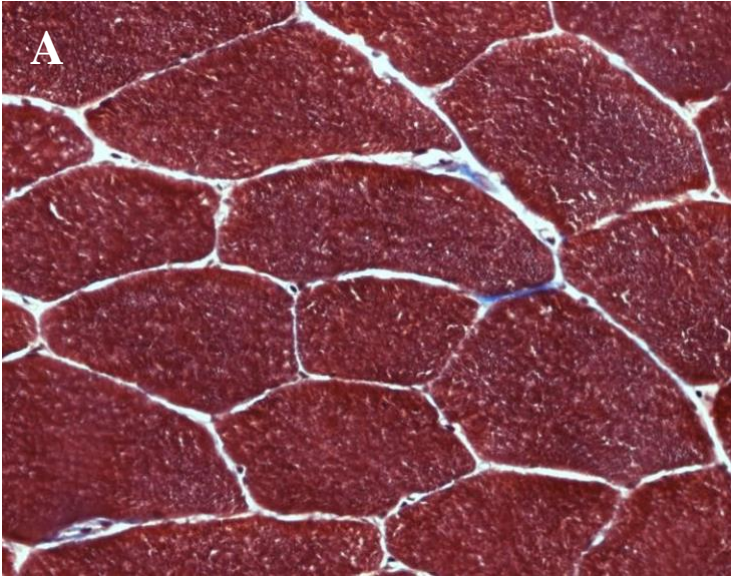


Figure 2



Caption here

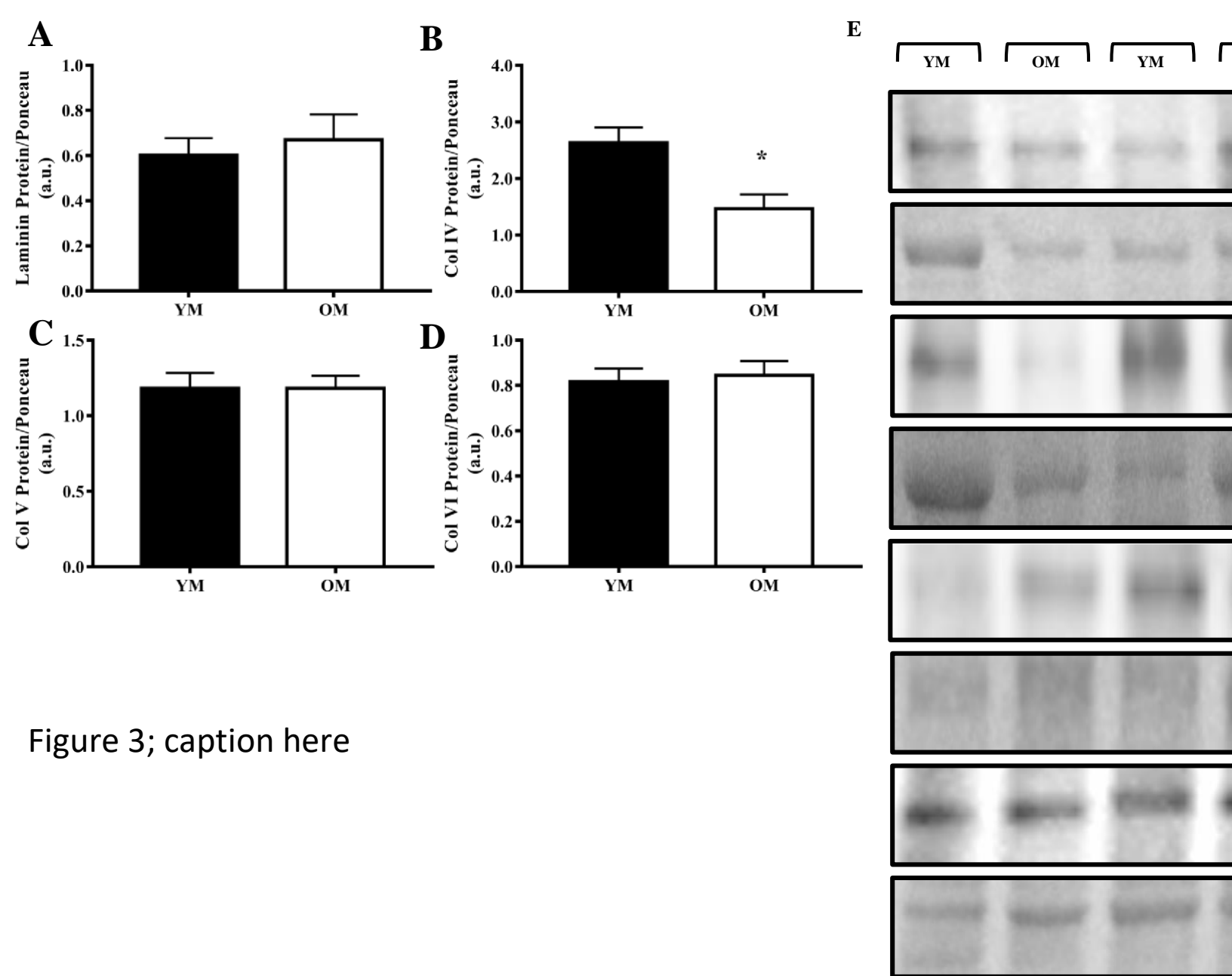
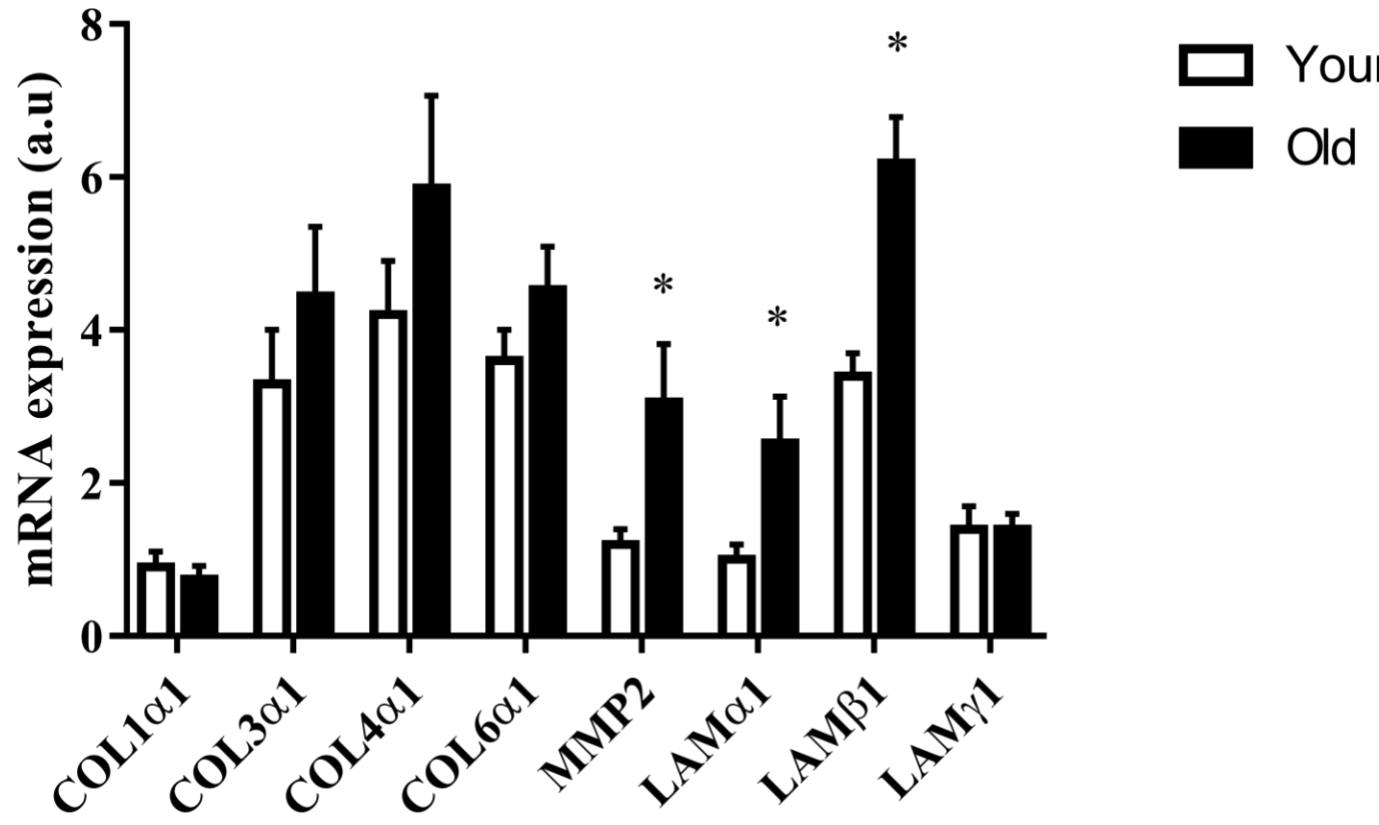


Figure 3; caption here

Figure 3



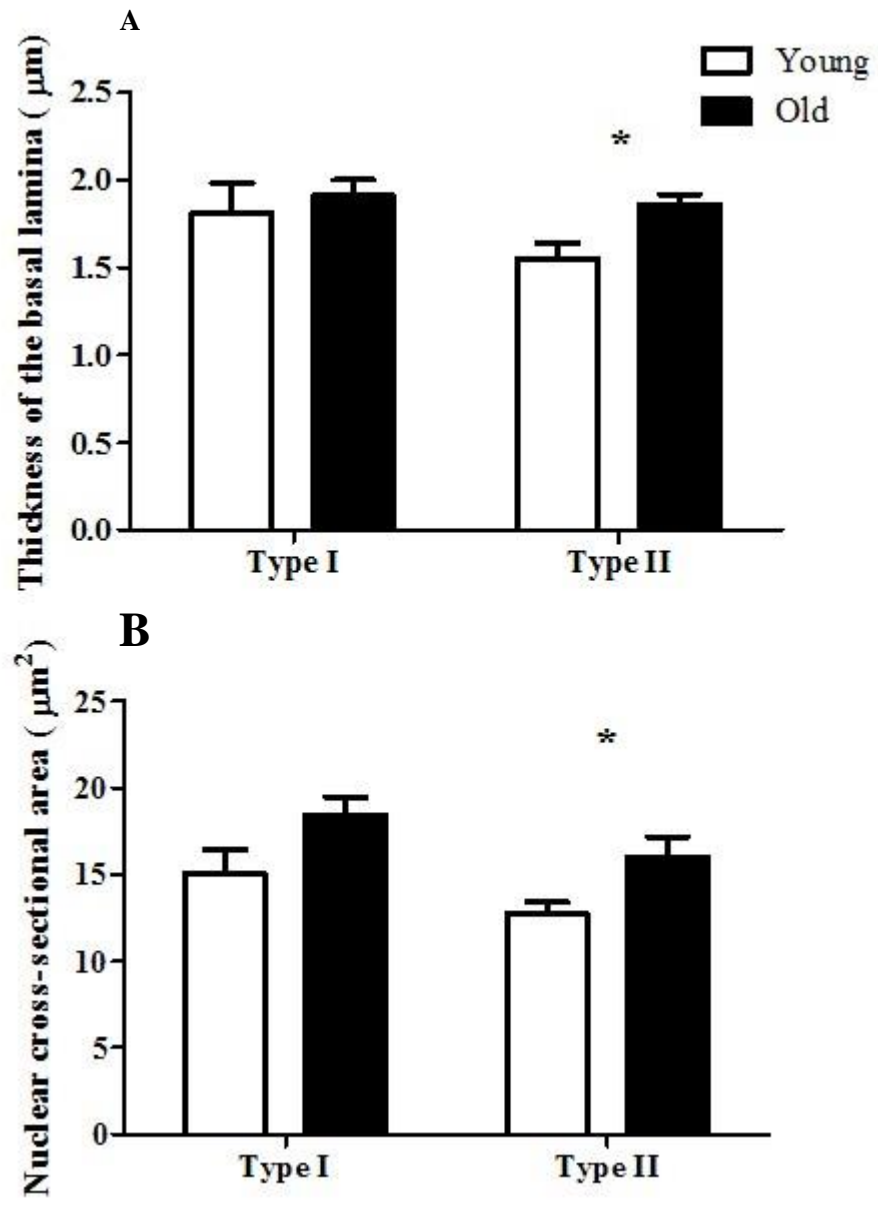
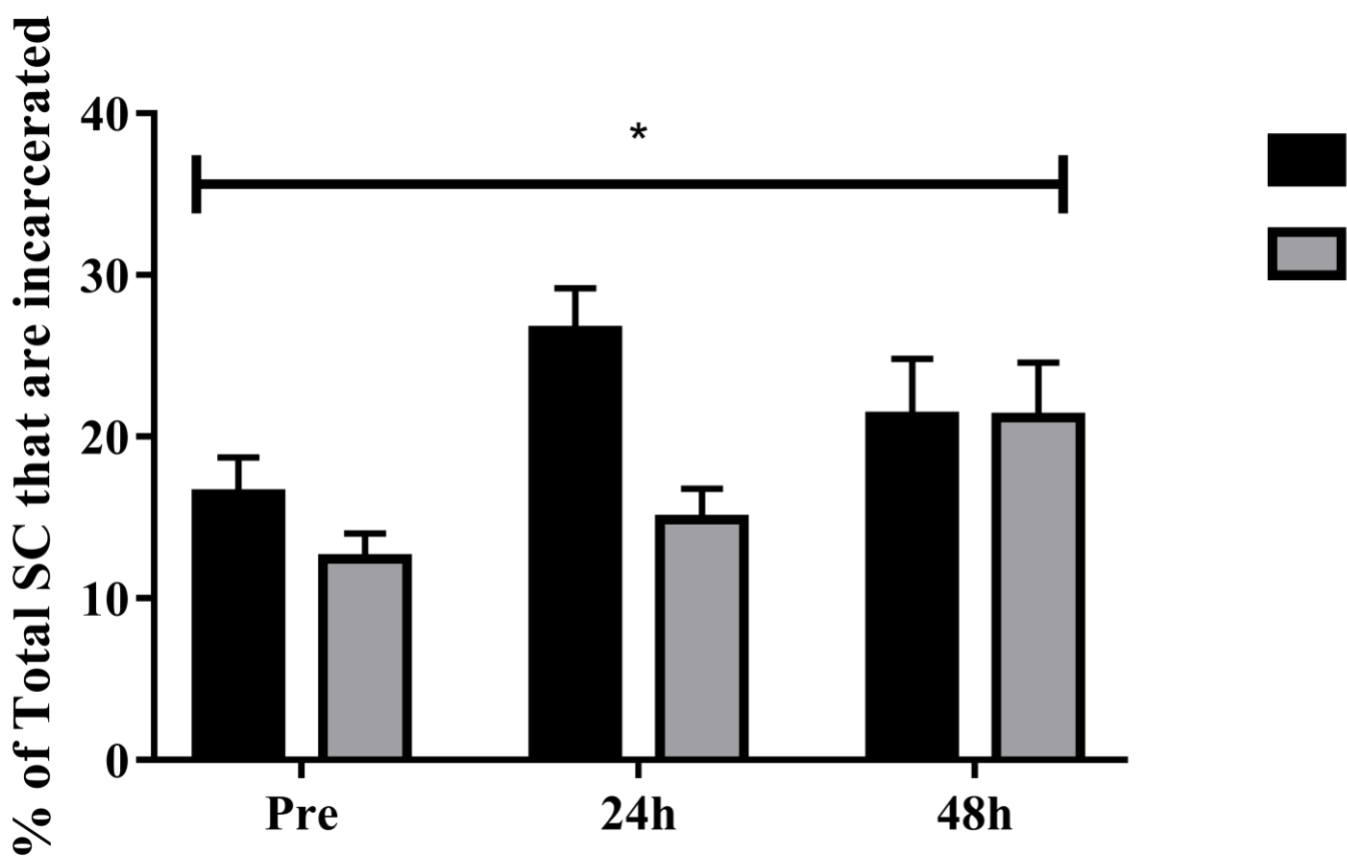
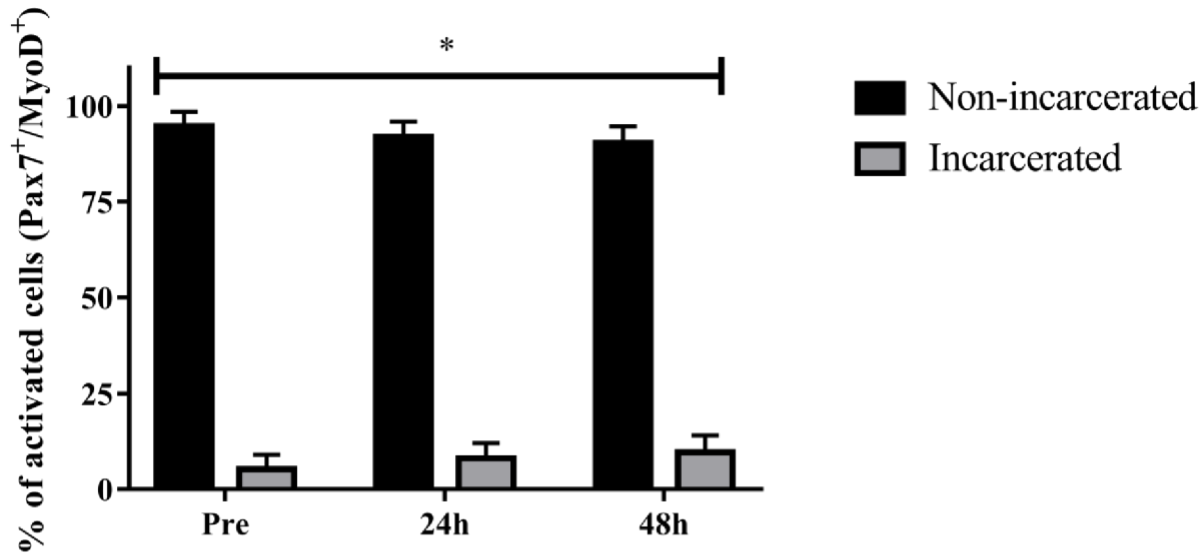
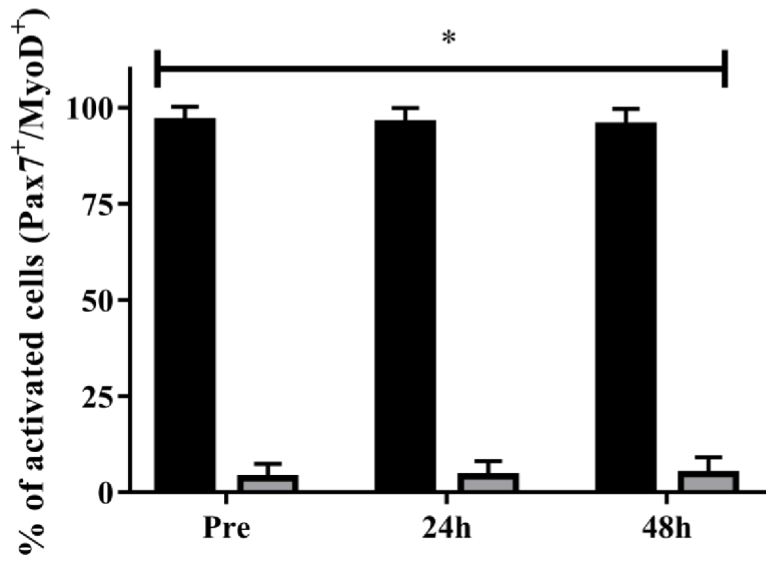
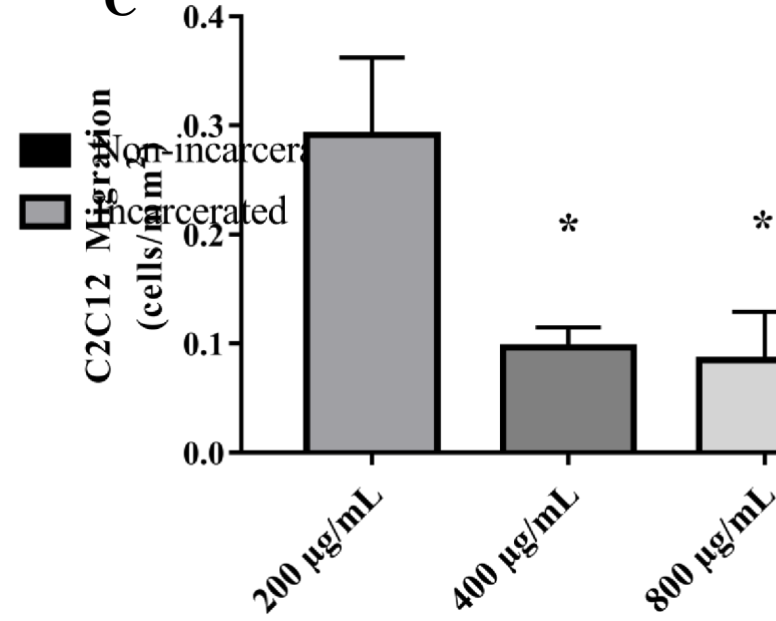


Figure 5

Figure 6

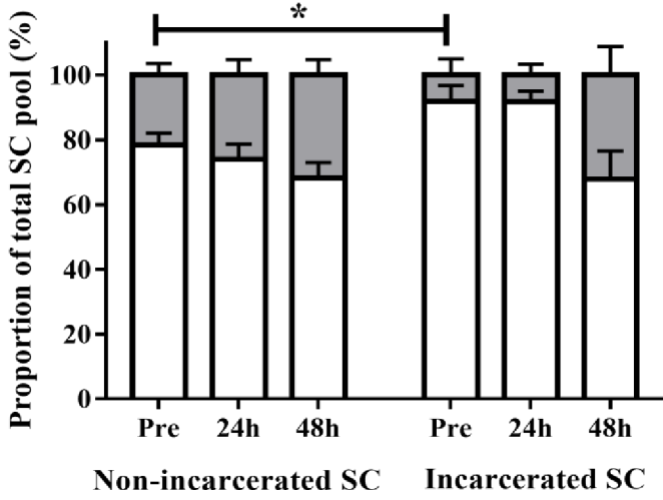


A Prior to 16 wks resistance training (PRE)**B** Following 16 wks resistance training (POST)**C**

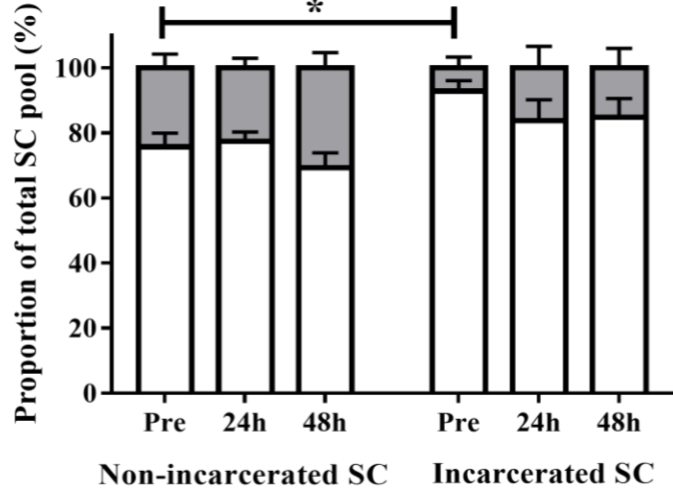
Prior to 12-wks combined exercise training

Following 12-wks combined exercise training

A

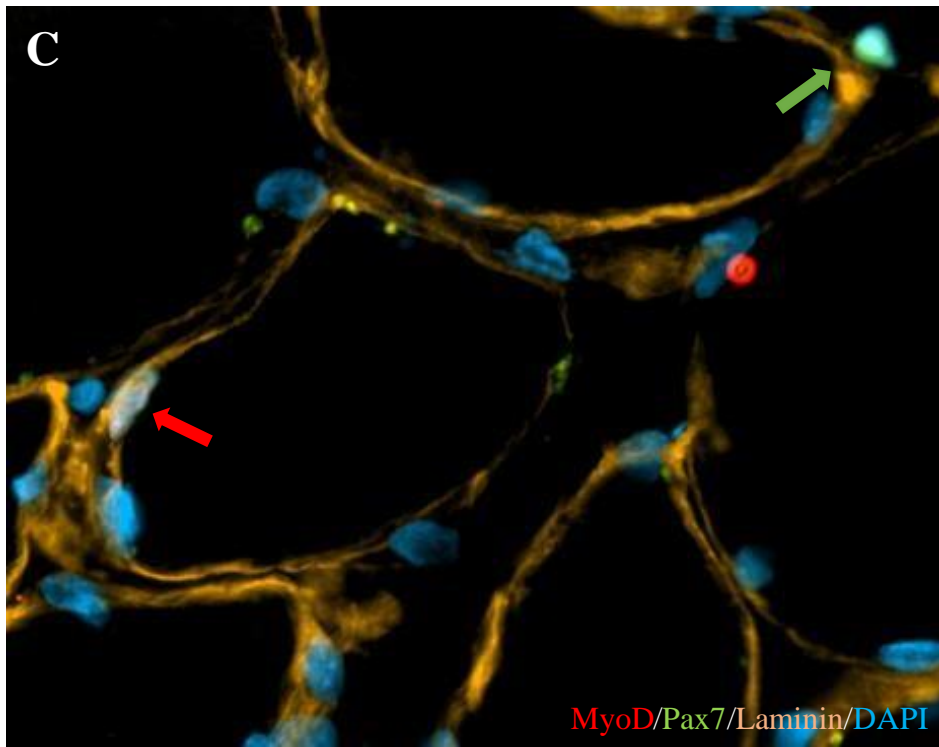


B

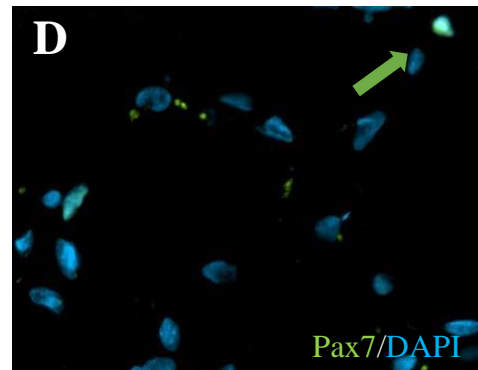


Active
Quiescent

C



D



E

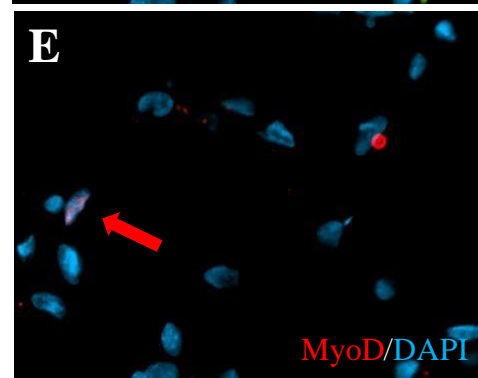


Figure 7

